Journal of Molecular Liquids 361 (2022) 119621

Contents lists available at ScienceDirect

Journal of Molecular Liquids

journal homepage: www.elsevier.com/locate/molliq

Thermodynamic properties of sodium deoxycholate at the gel-sol transition

Aida Jover [a,*], Jacobo Troncoso [b], Maria Chiara di Gregorio [c], Francisco Fraga López [d]

[a] Departamento de Química Física, Facultad de Ciencias, Universidade de Santiago de Compostela, Avenida Alfonso X El Sabio S/N, Lugo, 27002, Spain
[b] Departamento de Física Aplicada, Universidade de Vigo, Campus Ourense, 32004 Ourense, Spain
[c] Department of Chemistry, Sapienza University of Rome, P.le A. Moro 5, 00185 Rome, Italy
[d] Departamento de Física Aplicada, Facultad de Ciencias, Universidade de Santiago de Compostela, Avenida Alfonso X El Sabio S/N, Lugo, 27002, Spain

ARTICLE INFO

Article history:
Received 13 April 2022
Revised 2 June 2022
Accepted 12 June 2022
Available online 15 June 2022

Keywords:
Sodium deoxycholate
Bile salt
Sol-gel transition
Calorimetry
Densitometry
Electron microscopy

ABSTRACT

Sodium deoxycholate forms supramolecular aggregates in aqueous solution that are strongly dependent on temperature and pH. Upon fine tuning of these physicochemical parameters, two supramolecular aggregates can be achieved: a nanotubular phase having viscoelastic, gel-like, behavior and a sponge liquid phase. In this work, the thermodynamics of the transition between the two phases is characterized. Temperatures, volumes, and enthalpies of such transition have been experimentally determined using vibrating tube densitometry and differential scanning calorimetry. In addition, electron microscopy is used to follow the morphological transition between the two supramolecular structures. The dependencies of the thermodynamic properties with the pH and surfactant concentration of the solution are characterized, and the micrographs obtained from electron microscopy is used to explain the thermodynamics of the system.

1. Introduction

Natural bile salts are amphiphilic molecules considered as non-classic surfactants[1–3]. Unlike classic surfactants with a polar head attached to an apolar flexible chain, bile salts have a rigid steroid skeleton with three methyl groups, one or more hydroxyl groups, and a flexible chain that ends in a carboxylate group attached to this skeleton (see Fig. 1). The bifacial orientation of the polar and apolar substituents over the skeleton is responsible of their tensioactive behaviour in aqueous solution, including the formation of several structures, like micelles, nanotubes, or fibers, depending on the bile salt and experimental conditions.[2,4–10].

Common surfactants follow the aggregation model described by Israelachvili, [11,12] where different structures can be found: an isotropic phase in liquid solution at very low concentrations, micelles, rods, cubic or sponge phase, depending on the degree of ordering in their internal structure, lamellar phase, in which lamellar sheets, vesicles and nanotubes can be found, and the same structures as the former phases, but inverted at higher concentrations. The presence of a specific phase depends on the type of surfactant, its concentration, and the conditions of the external environment.

In this context, it was recently found that one of the natural bile salts, sodium deoxycholate (Fig. 1), shows an aggregation model in water that follows the behavior of classic surfactants [13]. A nanotube bundle phase with a self-standing gel consistency and a liquid sponge phase with a thixotropic phase change between them [14,15] were detected among the mesophases assembled by this bile salt. The hydrogel (nanotube bundles) are transformed into a liquid phase (sponge) as the pH or the temperature are increased (Fig. 1).

The behaviour of this gel has been extensively studied by X-ray, fluorescence, NMR and rheological techniques [14–20]. It must be pointed out that the observed structural changes for this bile salt appear in physicochemical conditions of high interest from a physiological perspective: aqueous solutions with a pH around 7 and slightly above room temperature, *i. e,* within the ranges where these molecules are involved in the living organisms[21–23]. In order to get a wider picture on the physical phenomena that are involved in this transition, and thus, to obtain a more precise modelling of the internal architectures that appear in this system, in

Abbreviations: NaDC, Sodium deoxycholate; HDC, deoxycholic acid; SAXS, Small Angle X-ray Scattering; WAXS, Wide Angle X-ray Scattering; TEM, Transmission Electron Microscopy; SEM, Scanning Electron Microscopy; T_t, temperature of transition; v, viscosity.

* Corresponding author.
E-mail address: aida.jover@usc.es (A. Jover).

https://doi.org/10.1016/j.molliq.2022.119621
0167-7322/

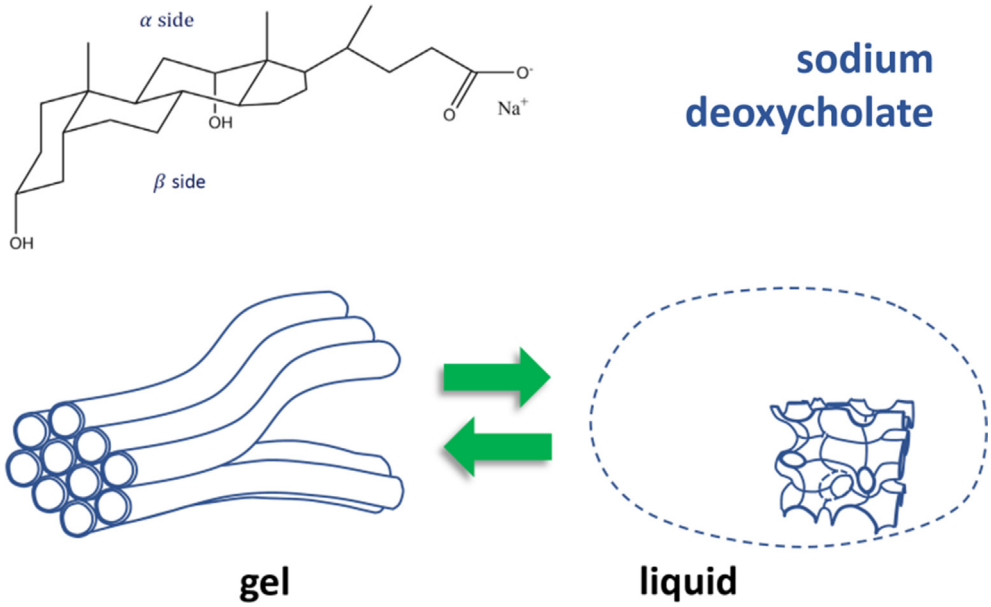

Fig. 1. Sodium deoxycholate mesophase transition between a self-standing gel (nanotube bundles) and a liquid solution (sponge phase) [13].

this work, a thermodynamic study of this gel-liquid phase change is carried out. In addition, new images of the microscopic structure of both phases are obtained from electron microscopy experiments. It must be noted that tiny variations in the external conditions of the medium triggers this mesophase change, and, therefore, this could be useful for future practical applications such as the dosage of poorly soluble drugs and their targeting or controlled release through the external stimuli modulation (pH or T) either physiologically or artificially controlled.

2. Experimental

Solutions were prepared by weighting the powders with a Mettler AE240 balance, having an estimated uncertainty of 0.1 mg. Besides sodium deoxycholate (NaDC), NaH_2PO_4 or Na_3PO_4 were also added to the solutions, since they stabilize the structure of the aggregates [13]. The pH was measured in a Jenway 3520 pH meter and adjusted by adding HCl or NaOH. The solutions were vigorously stirred to achieve homogeneity. Once the sample is prepared, gel consistence appears within 5–15 min. The gelling time is strongly dependent on the solution pH: the higher the pH value the longer the aggregation time.

2.1. Vibrating tube densimeter (VTD)

Density was measured using an Anton Paar VTD DMA5000. Uncertainty in these measurements is estimated in $1{\cdot}10^{-4}$ g·cm^{-3}, although much better reproducibility, around $2{\cdot}10^{-6}$ can be achieved [24]. Calibration was done using Milli-Q water and dry air. It is a well-known fact [24] that samples with high viscosity provoke a damping in VTDs oscillation that induces a wrong value of the density-the measured density is larger than the real one-, which must be corrected. This instrument performs automatically this correction, which is very relevant in the context of the present work. The gel solutions present a large viscosity, whereas the liquid ones are only slightly viscous. Therefore, the viscosity correction can be used as an experimental, very sensitive, probe to detect the transition between these two states. Since this instrument is designed to perform measurements for liquids, and the aggregated state has viscoelastic behavior, density measurements in this phase could show large uncertainties. This issue has been studied for different materials[25,26], concluding that this kind of densimeters are usually very reliable for viscoelastic samples. However, in order to check the results obtained with this apparatus, density measurements have been also performed in a dilatometer. It consists in an Erlenmeyer flask closed with a screw cap connected to a capillary tube with internal diameter of 1.9 mm, submerged in a thermostating bath. The dilatometer was calibrated with milliQ water, being its density taken from [27]. The solution density was determined by weighing and by measuring the position of the meniscus in the capillary. A comparison for some samples using vibrating densitometry and dilatometry has been carried out, finding excellent agreement, better than 0.00003 g·cm^{-3}. Therefore, only data from vibrating tube densitometry is included throughout the paper. Relative standard uncertainty in transition volume and uncertainty in transition temperature, T_t, are estimated in 7% and 3 K, respectively.

2.2. Differential scanning calorimeter (DSC)

Transition enthalpy of the solutions was determined using a DSC-Q20 from TA Instruments, Eschborn, Germany. Around 15 mg of sample was introduced in the closed aluminum experimental pan, whereas the same amount of water was used as reference. Experiments were performed at 2 K·min^{-1}, in the temperature interval (283.15 – 358.15) K giving 30 min of equilibration at the lowest temperature. Calibration of the instrument was carried out using Milli-Q water, being its fusion enthalpy data obtained from literature [28]. Relative standard uncertainty in transition enthalpy is estimated in ~ 8%.

2.3. Transmission electron microscopy (TEM)

TEM images were recorded on a JEOL JEM-1011 transmission electron microscope (80–100 kV) with a MegaView G2 camera. Samples were prepared by dropping solutions onto copper grids coated with Carbon-type A film. Excess water was removed by filter paper and the samples were dried at room temperature. Electron microscopy images of sponge-type phase and lamellar sheets were collected at a short exposure time to avoid damages

of the aggregates and their internal structure. The micrographs collected on these samples exhibit a dark contrast since low voltage electron intensity was used and due to an abundant presence of lamellar structures that covers the whole grid.

2.4. Cryogenic-transmission electron microscopy (cryo-TEM)

The vitrification process of the samples was performed with a FEI Vitrobot. A 3 ml drop of an aqueous solution of the samples was placed on a TEM Lacey carbon copper grid, the excess of water was blotted with filter paper and the grid was freeze-plunged into liquid ethane. Samples were then transferred under liquid nitrogen atmosphere to a Gatan TEM cryo-holder equipped with a liquid nitrogen reservoir. In this way, samples were handled and observed at T = 100 K. Cryo-TEM images were obtained in a Tecnai T20 (Thermofisher) with a working voltage of 200 KV and a CCD Veleta (lateral camera).

2.5. Scanning electron microscopy (SEM)

SEM and STEM images were recorded on a FESEM Ultra plus-ZEISS (20–30 kV). Images were collected using InLens, secondary electrons (SE), and STEM (transmission mode) detectors. Samples were prepared by placing a drop of samples on copper grids coated with Carbon-type A film, removing the excess solution with filter paper and air for drying them.

2.6. Cryogenic-scanning electron microscopy (cryo-SEM)

For the sample preparation, a drop of the solutions was deposited in a SEM holder and submerged into liquid nitrogen. The frozen samples were kept in liquid nitrogen and transferred by using a vacuum cryotransfer device (GATAN ALTO2100). Samples were freeze-fractured at − 120 °C and were observed at the same temperature in an JEOL JSM-6360LV by using a secondary electron detector (5 kV).

2.7. Crystalographic data

CCDC 1,123,586 (RbDC-H_2O (1/10)) [29], CCDC 1,247,414 (RbDC-H_2O (1/1)) [30], and CCDC 211,570 (HDC-H_2O (1/2)) [31] contain the supplementary crystallographic data used to assemble the related figures. These data can be obtained free of charge from The Cambridge Crystallographic Data Centre via www.ccdc.cam.ac.uk/structures.

3. Results and discussion

Density correction due to the sample viscosity $\Delta\rho$ was obtained from corrected, ρ_{corr}, and raw density data, ρ_{meas} from:

$$\Delta\rho = \rho_{meas} - \rho_{corr} \quad (1)$$

This correction is directly proportional to the viscosity, η, for samples with moderate viscosity. However, for η greater than around 700 mPa·s it remains almost constant, *i. e.* the damping effect over the vibrating period induces very small further density increments for $\eta \gtrsim$ 700 mPa·s [32–34]. Thus, the only region for which $\Delta\rho$ is sensible to variations in the sample viscosity is approximately the interval (10–700) mPa·s. It matches with the viscosity range where the studied transition takes place, because the sample viscosity strongly falls at the gel-sol transition. The transition temperature T_t was obtained as the temperature for which $\Delta\rho$ starts to fall from the plateau, as Fig. 2 shows for a representative sample.

There are some works [35,36] that have analyzed the density of NaDC solutions. However, the experimental conditions strongly differ from those of the present work, making a comprehensive comparison between both data sources not feasible. As a general comment, it can be said that the results are consistent with literature; the increment in density induced by the NaDC is around 0.0002 g·cm^{-3} per milligram of NaDC dissolved in 1 g of water. Viscosity and density of either gel [14–20] or liquid phases [36,37], have been previously studied, but measurements in experimental conditions close to the sol–gel transition have not been reported.

Molar volume of the sample v ($v = V/N$, N being the total number of moles of all species and V the total volume), was obtained from density data and it was subtracted from that of the solution without NaDC to observe the increment in molar volume Δv due to the creation or destruction of the aggregates. Fig. 2 shows the results for one of the studied samples. There, it is clearly shown that the gel-like system presents a smaller volume than the liquid one; *i. e.* gelling process involves a contraction of the system. Moreover, the transition does not seem to take place at one point, but in a range of temperatures of 5–10 K. To get a quantitative estimation of this transition volume, Δv_t, Δv below and above the transition was fitted to a straight line and the transition volume was obtained as the difference between both fits at the transition temperature (T_t). It must be pointed out that this transition volume is the difference between the two phases *per one mole of solution*, not per mole of the solute. It is worth to note that Δv in the liquid phase follows better the linear fit than in the gel, and, therefore, a narrower temperature range has been selected for the latter.

The transition enthalpy was obtained by integration of the heat capacity versus temperature curves. Fig. 3 shows the difference between the measured heat capacity and that of the baseline for a selected sample. There, it can be observed that the transition from gel to liquid state is endothermic; all studied solutions show this behavior. As above said, the transition seems to happen within a wide temperature range. Since the molecules need time to rearrange from tubes to sponge phases, and the calorimetric measurements are dynamic, *i. e.* temperature is not stable, but a temperature ramp is applied, the transition enthalpy is extended over a large temperature range. This is significantly wider that those obtained from density measurements, where the effects of the transition kinetics are mostly excluded. This makes the traditional methods to determine phase change temperatures from calorimetry to be inaccurate. Therefore, these measurements are used only to evaluate the transition enthalpy, and not for the T_t, which was obtained from the viscosity estimations.

As commented in the introduction, pH has a strong effect on the appearance of the highly ordered structures observed for these solutions. As a result, their thermodynamic properties are also strongly influenced by the pH. Fig. 4 and Table 1 show T_t versus pH for the studied samples. A clear negative correlation with the pH is observed. T_t drops from 316 K at pH = 6.76 to 298 K at pH = 7.24 for NaDC and NaH_2PO_4 concentrations of 40 mM and 20 mM, respectively. For larger pH values, the gel phase does not appear, and for pH values lower than 6.7, the solution is no longer stable, and a precipitate is observed. If sodium deoxycholate or NaH_2PO_4 concentrations are increased to 80 mM and 60 mM, respectively, the T_t raises, as shown in Fig. 4, being the lines of T_t versus pH almost parallel to those of [NaDC] = 40 mM and [NaH_2PO_4] = 20 mM. The effect of increasing the NaH_2PO_4 concentration is comparable to rising the NaDC concentration. Besides being T_t higher, these solutions are in gel phase over a larger pH range, obtaining stable structures up to pH around 7.5.

Fig. 5 and Table 1 show the transition volume versus pH. This quantity hardly varies with any of the controlled physical parameters: almost all solutions have shown quite similar transition volumes, ~0.004 cm^3·mol^{-1}, irrespective of the NaDC and NaH_2PO_4

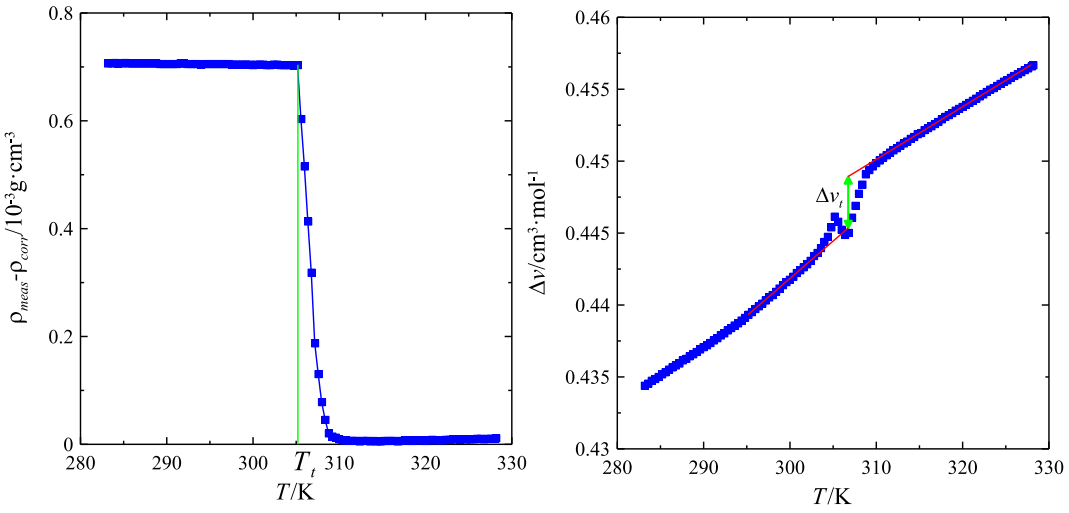

Fig. 2. Left.- Density correction (blue squares) and transition temperature obtained from these data (marked with the green line). Right.- Difference between the sample molar volume and that of the solution without NaDC, blue squares: experimental data; red line: fits in the liquid and gel phases. Sample with [NaDC] = 80 mM, [NaH_2PO_4] = 20 mM and pH = 7.34.

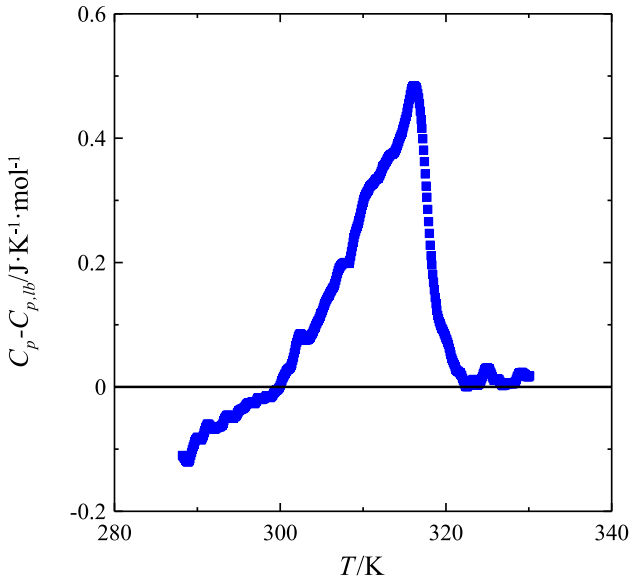

Fig. 3. Difference between the sample heat capacity and that of the base line for the sample with [NaDC] = 80 mM, [NaH_2PO_4] = 20 mM and pH = 7.32. This sol–gel transition shows endothermic behavior.

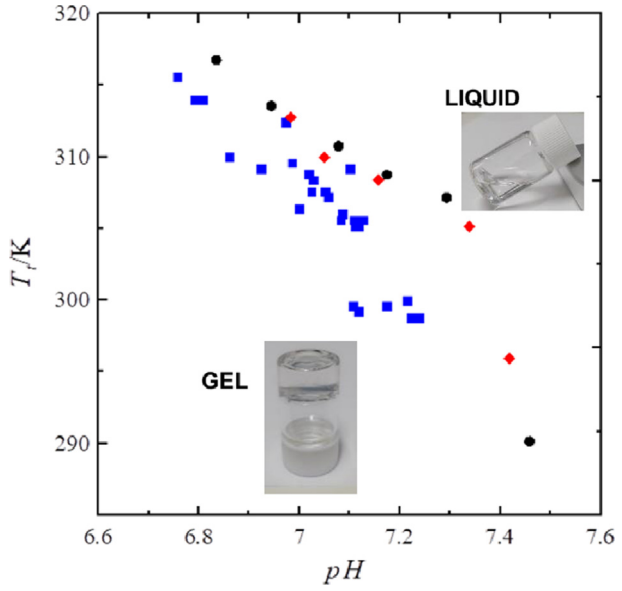

Fig. 4. Transition temperature T_t as a function of pH for the studied samples: blue squares [NaDC] = 40 mM, [NaH_2PO_4] = 20 mM; red diamonds [NaDC] = 80 mM, [NaH_2PO_4] = 20 mM; black circles [NaDC] = 40 mM, [NaH_2PO_4] = 60 mM.

concentrations and pH value. Only for the most basic solutions (pH > 7.4), a clear drop in Δv_t is observed. Fig. 6 and Table 2 show the transition enthalpy versus pH for the studied solutions. As done for transition volume, this quantity is given by mole of solution, not for mole of the solute. The results are quite similar to those found for T_t, a clear negative correlation with the pH is observed and increasing the NaDC or NaH_2PO_4 concentration makes the enthalpy to raise. It is worth to note that the obtained values, are of the same order of the micellization enthalpies for the NaDC [38,39].

Although thermodynamic data provide very important information about the physics of the transition, having information about the microscopic structures that form the observed phases would enrichen the understanding of the observed behavior for these systems. Moreover, it would allow to relate the microscopic picture with the thermodynamics of the system. Fortunately, recently [13], it has been shown that this is possible, and electron microscopy images in similar conditions to those studied here have been reported. Fig. 7 shows new images of the supramolecular structures existing in both phases. An intermediate state in the phase transition from the sponge to the nanotube bundles phase is shown in Fig. 8. The structure of the gel can be observed in these pictures: bundles of nanotubes form this phase (panels a-b of Fig. 7). On the other hand, the panels d-f of Fig. 7 clearly show that the liquid phase retains some structure; it is not a simple liquid, but a sponge phase. The system would be made up of deoxycholate bilayer structure packed in a back to back way, with the apolar surface (α side) towards the inside of the membrane and the polar area surface (β side) and the side chain with its counterion fraction, towards the aqueous environment. Such a molecular model was previously discussed by crossing Small and Wide X ray Scattering (SAXS-WAXS), single crystal X-ray structures and different electronic microscopies [11,13,30]. This liquid phase does not present high organization at the molecular level like the linking of the nan-

Table 1
Transition temperature T_t and volume Δv_t for the studied solutions at different deoxycholate and disodium phosphate molarities [NaDC] and [Na_2HPO_4].

pH	T_t/K	Δv_t /cm^3·mol^{-1}	*pH*	T_t/K	Δv_t /cm^3·mol^{-1}
[NaDC] = 40 mM, [NaH_2PO_4] = 20 mM			[NaDC] = 40 mM, [NaH_2PO_4] = 20 mM		
6.76	316	0.0041	7.12	299	0.0042
6.79	314	0.0047	7.13	306	0.0039
6.81	314	0.0042	7.17	300	0.0048
6.86	310	0.0036	7.22	299	0.0039
6.93	309	0.0041	7.22	300	0.0048
6.98	312	0.0041	7.24	299	0.0041
6.99	310	0.0042	[NaDC] = 80 mM, [NaH_2PO_4] = 20 mM		
7	306	0.0036	6.98	313	0.0049
7.02	309	0.0038	7.05	310	0.0049
7.03	308	0.0038	7.16	308	0.0041
7.03	308	0.0039	7.34	305	0.0038
7.05	308	0.0039	7.42	296	0.0025
7.06	307	0.0039	[NaDC] = 40 mM, [NaH_2PO_4] = 60 mM		
7.08	306	0.0037	6.84	317	0.0045
7.09	306	0.0036	6.94	314	0.0043
7.11	305	0.0040	7.08	311	0.0041
6.93	309	0.0041	7.17	309	0.0039
6.76	316	0.0041	7.29	307	0.0044
7.05	308	0.0039	7.46	290	0.0009
6.79	314	0.0047			

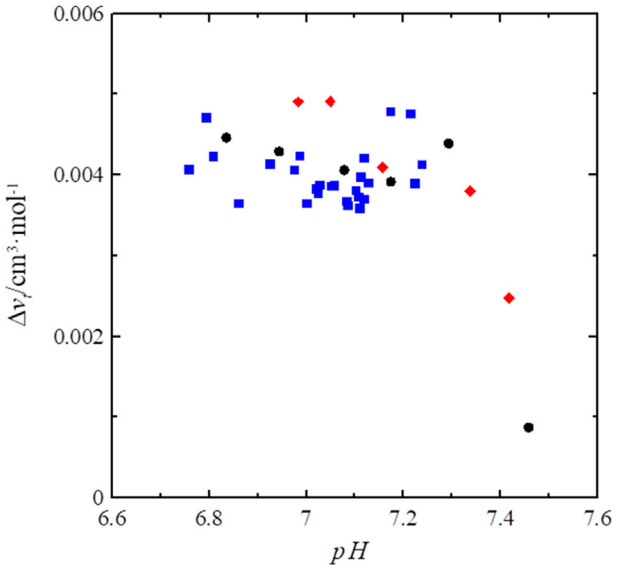

Fig. 5. Transition volume Δv_t as a function of pH for the studied samples: blue squares [NaDC] = 40 mM, [NaH_2PO_4] = 20 mM; red diamonds [NaDC] = 80 mM, [NaH_2PO_4] = 20 mM; black circles [NaDC] = 40 mM, [NaH_2PO_4] = 60 mM.

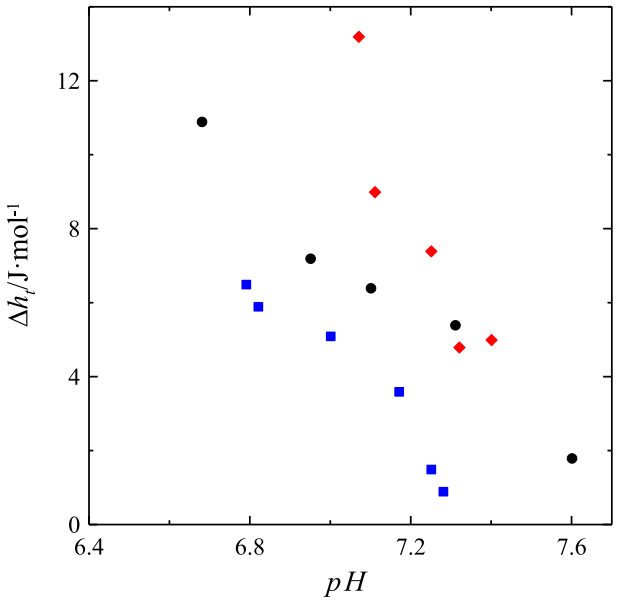

Fig. 6. Transition enthalpy Δh_t as a function of pH for the studied samples: blue squares [NaDC] = 40 mM, [NaH_2PO_4] = 20 mM; red diamonds [NaDC] = 80 mM, [NaH_2PO_4] = 20 mM; black circles [NaDC] = 40 mM, [NaH_2PO_4] = 60 mM.

otubes [13,29,40]. Nanotubes and sponge arrangements in both phases coexist with lamellar sheets as can be seen in the cryo-SEM photographs (panels c and f of Fig. 7). It must be noted that the liquid phase in Figs. 7 and 8 is shown at ambient temperature. This has been accomplished by increasing the pH (see Figure captions). In a previous paper, [13] it has been demonstrated that the effect of the pH increasing on the gel is similar to the effect induced by the temperature increase (transitions observed at pH values from 7.0 to 7.6 or temperatures from 20 °C to 40 °C). Therefore, the same structures would be observed for the liquid phase at higher temperatures.

The detailed molecular structure of the nanotube is hardly detected from the electron microscopy images. However, recent SAXS data of the gel-like system [13] suggest elongated structures that present six sharp peaks in the WAXS range 0.83–0.50 nm, thus indicating a relevant degree of molecular order inside the aggregates. Five of these signals are similar to the spacings of a hexagonal arrangement of 8/1 trimer helixes observed by Giglio *et al* [40–42] in solid state fibers drawn from NaDC gels. The highly organized arrangement at the molecular level along with the electron and optical microscopy techniques strongly suggest that nanotube bundle structures describe the gel mesophase. Fig. 9 displays a molecular model for the nanotubes [13], built up from the two crystal structures of monoclinic [30] and hexagonal [29] rubidium deoxycholate (RbDC). This salt was used instead of NaDC because attempts to determine the NaDC crystal structure were unsuccessful. However, it has been confirmed that in the NaDC crystal has helices and hexagonal structure, very likely identical to the RbDC as Giglio *et al* confirmed [28,31,33]. The evident chemical similarities between both salts, avails that the results for the RbDC can be extrapolated to NaDC. Assuming structure similarity in both helixes (gel and solid state), a water channel should exist inside

Table 2
Transition enthalpy Δh_t for the studied solutions at different deoxycholate and disodium phosphate molarities [NaDC] and [Na_2HPO_4].

pH	Δh_t /J·mol^{-1}	*pH*	Δh_t /J·mol^{-1}	*pH*	Δh_t /J·mol^{-1}
[NaDC] = 40 mM [NaH_2PO_4] = 20 mM		[NaDC] = 80 mM [NaH_2PO_4] = 20 mM		[NaDC] = 40 mM, [NaH_2PO_4] = 60 mM	
6.79	6.5	7.07	13.2	6.68	10.9
6.82	5.9	7.11	9.0	6.95	7.2
7.00	5.1	7.25	7.4	7.10	6.4
7.17	3.6	7.32	4.8	7.31	5.4
7.25	1.5	7.40	5.0	7.60	1.8
7.28	0.9				

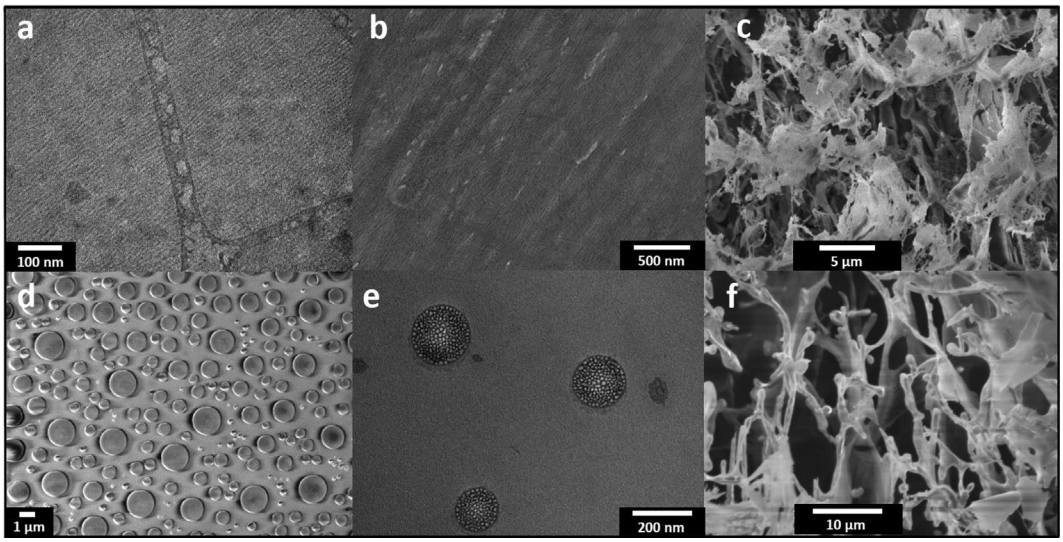

Fig. 7. a) Cryo-TEM, b,e) TEM, **e)** SEM **c,f)** Cryo-SEM images of representative aggregates found in sample for **a)** [NaDC] = 80 mM pH = 7.36, gel **b)** [NaDC] = 40 mM, [NaH_2PO_4] = 20 mM, solution pH 7.00, gel. **c)** [NaDC] 85 mM NaH_2PO_4 20 mM, pH 7.45, gel. **d)** [NaDC] 80 mM, NaH_2PO_4 20 mM pH 11.65, liquid. **e)** [NaDC] = 20 mM, pH 11.84 NaH_2PO_4 20 mM, liquid. **f)** [NaDC] = 40 mM NaH_2PO_4 50 mM, pH 9.15 liquid. T = 20 °C. a-c images correspond to the gel-like phase made of nanotube bundles and c-f to the liquid (sponge) phase. Lamellar sheets coexist with both phases and can be seen in c-f micrographs.

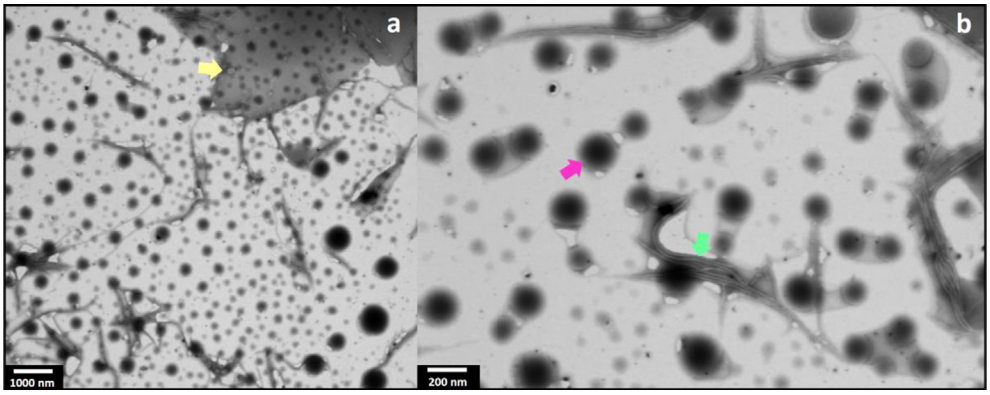

Fig. 8. STEM images of representative aggregates found in NaDC 80 mM pH 11.65 NaH_2PO_4 20 mM, T = 20 °C. Lamellar sheets (yellow arrow), sponge phase (pink arrow) and initial nanotube bundles (green arrow).

the helix connecting the nanotubes in the gel phase. This helix would be hydrophilic in his inner part and apolar in the external surface, as Fig. 9 shows. The channel should have inside a minimum of 3.6 water molecules for each deoxycholate anion (crystal data [30]) and might coexist with a Na^+ cation for neutrality. The water molecules inside the NaDC channel should be less organized than in the crystal, but more structured than water molecules in the bulk solution. Ion-ion, ion–dipole interactions, and a network of hydrogen bonds placed inside the helix are the forces that stabilize this structure [29]. As shown in Fig. 9, this helix acts as a joint between the nanotubes and it is, in last term, the main responsible for the appearance of the gel phase. This structure can be considered as the precursor of the hexagonal crystalline arrangement of NaDC in solid state [29,40,41].

A pH decrease in the global system increases the fraction of the protonated bile salt (deoxycholic acid, HDC) [43]. From the perspective of each single molecule, when the deoxycolate anion captures a hydrogen ion, the negative global charge of the molecule is cancelled, the polarity distribution of the molecule areas changes, diminishing the Hydrophilic-Lipophilic Balance (HLB) [44]. The polar and apolar molecular areas are now modified and the molecules will be reorganized inside the aggregates bilayer, remodelling

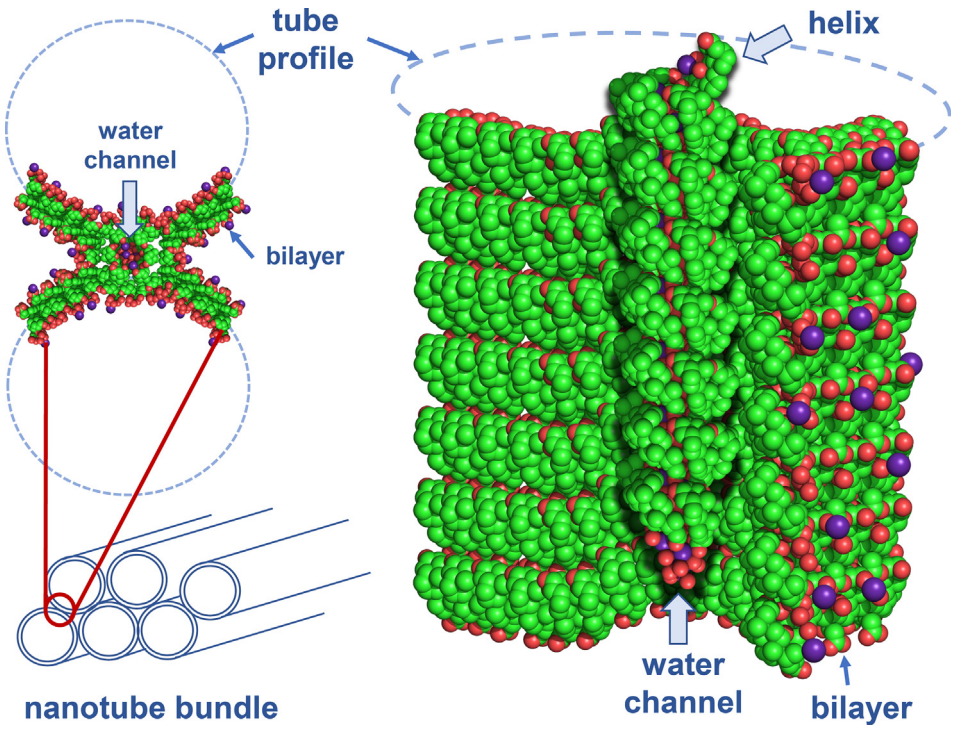

Fig. 9. Molecular model for the NaDC nanotube bundles and the tubes junction[13]. Bilayer in the real structures would present certain molecular disorder. The helix connecting the nanotubes would have a similar structure to that of the Fig. 3D models were constructed from the crystal structures of monoclinic [30] and hexagonal [29] RbDC.

its internal and external parts[11–13] as well as the intermolecular forces that hold the aggregates. Small changes in the HLB can produce great variations in the external shape of the lamellar structures [12], and the neutralization of a fraction of NaDC molecules in the membrane should vary the external shape. HDC has a low solubility in water at acidic pH [45], and, therefore, there is a limit in the amount of HDC molecules that can be rearranged in the bilayer structure before HDC precipitates. The creation of the helicoidal structure inside the membranes, shown in Fig. 9, allows NaDC molecules to be kept in solution in its ionic form. Coherently, it has been found out that the helix formed by NaDC is more stable at low pH, and therefore, the NaDC conversion into HDC does not happen inside the channel [40]. As a consequence, the fraction of NaDC assembling the water channel is protected from the hydrogen exchange and can be maintained in the structure of the transparent gel system. The infinite nanotubes organization in the gel-like system gives rise to a tricontinuous phase [12] where three different percolation channels coexist: the microenvironment inside the tubes, the bulk solution, and the bilayer that form the nanotubes; this allows the solubilization of the HDC molecules for taking place in a much greater extent than in the bulk.

The thermodynamic measurements shown in Figs. 4-6 reveal that two clear different phases are observed, the gel at low temperature and pH and the liquid at high pH and temperature. By making use of $\Delta u_t = \Delta h_t - p\Delta v_t$ it can be concluded that the contribution to the change in internal energy Δu_t comes mainly from enthalpy, since the term $p\Delta v_t$ is around 0.0004 J·mol^{-1}, ten thousand times smaller than the typical values found for Δh_t. Thus, internal energy is more positive for the liquid, a fact that reveals that, as expected, molecular interactions are stronger in the gel phase. Moreover, considering that at constant pressure the Gibbs free energy variation, Δg_t, is 0 at the phase transition, since $\Delta g_t = \Delta h_t - T\Delta s_t$, the transition entropy Δs_t must be positive. As a result, the disorder increases in the gel-sol transformation. This is also coherent with the molecular model in Fig. 9 for the gel structure: a more ordered self-assembly helical structure of deoxycolate ions and an ordered water channel inside, differing from the more random bilayer that generates the sponge phase.

The sol–gel transition occurs in different systems where the gelation is carried out through processes that differ substantially at the molecular level. Examples of these systems in liquid solutions are the connection of polymers generating a three-dimensional network through covalent bonds [46,47] or weak interactions, as hydrogen bonds, [48] where ions or small molecules can be involved [49]. This transition may also be related to a change of the supramolecular structures including self-assembled architectures as rods, sheets or nanotubes [50,51]. All these processes can modify the viscoelastic properties of the whole system and they are the main mechanisms which contribute to the enhancement of the viscosity in gels. Traditionally, gels have been divided into two classes: strong or quenched, and weak or annealed [52], being the gelation irreversible for the former and reversible for the latter. The studied deoxycholate systems belong to the annealed gels, since gelation are made up through hydrogen bonds and other weak interactions, being reversible as previous works have shown [14–19].

The first theoretical models of gelation, based in percolation concepts [53–56], had considered the sol–gel transition as purely geometric; therefore, no singularities in the free energy would be expected. Thus, typical phase transition magnitudes, like transition enthalpy or volume, would not make sense. Later works, which used more elaborated concepts based on percolation theory, led to the conclusion that quenched gels do show singularities in its free energy [57–61] but annealed gels do not [59,62]. Nonetheless, it has been argued [63,64] that this is not correct, because the contribution of large and complicated cyclic clusters to the free energy, previously neglected, should have been considered. As a result, the gel-sol transition even in weak gels would be a genuine thermal phase transition, in fact, a first-order phase transition [63]. In any case, the nature of the sol–gel phase change is nowadays an open subject and a complete understanding of this transition is still lacking [65].

The experimental results reveal that the observed transition has changes both in the volume and enthalpy, that is, it is first-order. On the other hand, the electron microscopy images reveal that nanotubes are observed in the gel, but they disappear in the liquid phase. Therefore, this nanotube vanishing must have a contribution to the transition volume and enthalpy. If the sol–gel phase transition would be purely geometric, the change in the thermodynamic properties, *i. e.* the transition enthalpies and volumes, could not be due to this gel-sol phase change and, therefore, Δv_t and Δh_t would come from the transition between two supramolecular structures (from nanotubes to sponge phase). Under this hypothesis, the gel would appear due to the self-assembly of the nanotubes in a three-dimensional structure; when nanotubes vanish, the sponge phase would emerge. Thus, the observed changes in the enthalpy and volume would come only from the destruction of the nanotubes, and it would not be directly related to a gel-sol transition. Therefore Δv_t and Δh_t would be considered as thermodynamic properties that would correspond to the transformation of the nanotube-bundled structure that forms the gel into the sponge phase. However, if the transition from sol to gel is not purely geometric, but it would imply some discontinuities in the free energy -*i. e.* it is a first-order phase transition- this does not apply. In this case, there would be two contributions to the transition volume and enthalpy one due to the sol–gel transition, and the other one to the nanotube destruction. Distinguishing which amount belong to the transition and which one to the nanotube destruction is not an affordable task with the available precision of the present experimental methods.

The results for T_t and enthalpy (Figs. 4 and 6) clearly show the enhancement of the supramolecular structures as the solution becomes more acidic, since both T_t and Δh_t increases as pH decreases. This perfectly fits the above cited explanation about the nanotube assembly: low pH values make the concentration of the protonated bile salt to increase, modifying the hydrophilic-lipophilic balance, and making more stable the helix that links the nanotubes. Therefore, the nanotube phase becomes more stable at low pH, and, as a consequence of this, the difference in the energy between this phase and the sponge one becomes higher, reverting in larger transition enthalpies as pH becomes lower. This also explain the decrease in T_t with the pH: since the nanotube structure is more stable at low pH, higher temperature is needed to destroy it. The same tendency is attained if, instead of decreasing pH, NaDC or NaH_2PO_4 concentration is raised, although this effect is significantly more marked for the former: doubling [NaDC] has almost the same effect than tripling [NaH_2PO_4]. This is what is expected, since the NaDC form the nanotubes, and NaH_2PO_4 plays only an adjuvant role in developing these supramolecular structures [17]. These results match previous findings regarding the rheological behaviour of this system [19], since the gel strength follows the same trends. Therefore, any of these factors –acidity of the solution and NaDC or NaH_2PO_4 concentrations- promotes the formation of the nanotubes bundles, which makes the gel to become a more structured system, as the raise in T_t and Δh_t shows. As for the volume changes between the gel and liquid phase, this effect is much milder (*cfr.* Fig. 5). The volume contraction due to the formation of the nanotube bundles is almost independent of the pH or NaDC or NaH_2PO_4 concentration; only for $pH > 7.2$ Δv_t clearly decreases. Therefore, one can conclude that the effect of the gel structure enhancement over the volume contraction is only relevant when the system is very disordered, that is, at large pH. Further pH decrements strengthen the gel structure, but they do not have a relevant effect over the volume contraction of the system.

Finally, it is interesting to point out that, for a given pH, Δh_t is around twice larger for the solutions with [NaDC] = 80 mM than for [NaDC] = 40 mM. This implies that, if the enthalpy is calculated per NaDC mole, instead of per solution mole, quite similar values are obtained for both concentrations. Therefore, the bonding energy between the NaDC molecules that form the nanotubes are not significantly affected by the NaDC concentration. However, this does not hold for Δv_t: since it does not change with NaDC composition, if we consider the transition volume per NaDC molecule, we get values twice larger for the solutions with [NaDC] = 40 mM. A feasible explanation could be a shift in the equilibrium towards the lamellar sheets coexisting with the bundles in the gel as the NaDC concentration rises. The NaDC molecules of the bilayer sheets would have a similar volume per molecule as the sponge phase as they do not have the helical structure.

4. Conclusions

The thermodynamic and structural analysis of sodium deoxycholate in aqueous solution presented in this work gives new insights about the supramolecular structures that these solutions present. The gel state is formed by nanotubes bundles that form a three-dimensional structure over the whole system, whereas the liquid state is a sponge phase. The density measurements show that the volume difference between the gel and the liquid phases is almost independent on the pH; only for the most basic solutions a clear decrement in the transition volume can be observed. However, both transition temperature and enthalpy do vary with pH, signifying that, although the structure of the sample would be quite the same, it is weaker as pH raises: temperature breaks easier the structure as pH becomes larger –lower T_t and as pH increases-, and the energetic difference between gel and liquid phases is also smaller as pH increases –lower Δh_t as pH raises. Therefore, the general picture that can be extracted from these thermodynamic analyses is that, although pH hardly affects the volumetric behavior of the gel state, it strongly affects its strength and stability.

It is important to emphasize that unlike certain classes of materials as polymers [66], the transition enthalpy values between different phases of surfactants [67–71], and even more not classical surfactants, are uncommonly reported. As concerns bile salts, to the best of our knowledge, transition enthalpy data have been reported only for few derivatives [72,73] but not for pure bile salts. Therefore, future experimental work devoted to the study of the thermodynamics of these compounds would give new insights that could help to get a better understanding of the physicochemical behavior of these systems.

CRediT authorship contribution statement

Aida Jover: Conceptualization, Methodology, Investigation, Data curation, Writing – review & editing. **Jacobo Toncoso:** Conceptualization, Methodology, Investigation, Data curation, Writing – review & editing. **Maria Chiara di Gregorio:** Formal analysis, Writing – review & editing. **Francisco Fraga López:** Methodology.

Declaration of Competing Interest

The authors declare that they have no known competing financial interests or personal relationships that could have appeared to influence the work reported in this paper.

Acknowledgements

Funding for the present work was provided by the Ministerio de Economía, Industria y Competitividad, Spain (Grant number MAT2017-86109-P), Ministerio de Ciencia y Tecnología, Spain

(Grant number PID2020-115722 GB-C22) and European Synchrotron Radiation Facility (ALBA) for the project 2021024910 (2021). We acknowledge to Servicio General de Apoyo a la Investigación-SAI, Universidad de Zaragoza. M. C. di Gregorio acknowledges support from the programme "Rita Levi Montalcini for young researchers" of the Italian Ministry of University and Research. Funding for open access charge: Universidade de Santiago de Compostela/CRUE/CISUG.

References

[1] D. Madenci, S.U. Egelhaaf, Self-assembly in aqueous bile salt solutions, Curr. Opin. Colloid Interface Sci. 15 (1-2) (2010) 109–115, https://doi.org/10.1016/j.cocis.2009.11.010.
[2] M.C. di Gregorio, L. Travaglini, A. Del Giudice, J. Cautela, N.V. Pavel, L. Galantini, Bile Salts: Natural Surfactants and Precursors of a Broad Family of Complex Amphiphiles, Langmuir. 35 (21) (2019) 6803–6821, https://doi.org/10.1021/acs.langmuir.8b02657.
[3] L. Galantini, M.C. di Gregorio, M. Gubitosi, L. Travaglini, J.V. Tato, A. Jover, F. Meijide, V.H. Soto Tellini, N.V. Pavel, Bile salts and derivatives: Rigid unconventional amphiphiles as dispersants, carriers and superstructure building blocks, Curr. Opin. Colloid Interface Sci. 20 (3) (2015) 170–182, https://doi.org/10.1016/j.cocis.2015.08.004.
[4] D.M. Small, Size and structure of bile salt micelles. Influence of structure, concentration, counterion concentration, pH, and Temperature, Adv. Chem. Ser. 84 (1968) 31–52, https://doi.org/10.1021/ba-1968-0084.ch004.
[5] H. Kawamura, Y. Murata, T. Yamaguchi, H. Igimi, M. Tanaka, G. Sugihara, J.P. Kratohvil, Spin-label studies of bile salt micelles, J. Phys. Chem. 93 (8) (1989) 3321–3326, https://doi.org/10.1021/j100345a087.
[6] J. Jover Ramos, Aida., Meijide del Río, F., Rodríguez Núñez, E.; Vázquez Tato, Aggregation behavior of bile salts. Recent Res. Dev. Phys. Chem., 1999.
[7] A.R. Campanelli, S. Candeloro De Sanctis, E. Giglio, N. Viorel Pavel, C. Quagliata, From crystal to micelle: A new approach to the micellar structure, J. Incl. Phenom. Mol. Recognit. Chem. 7 (4) (1989) 391–400, https://doi.org/10.1007/BF01079774.
[8] S. Mukhopadhyay, U. Maitra, Chemistry and biology of bile acids, Curr. Sci. 87 (2004) 1666–1683, https://doi.org/https://www.jstor.org/stable/24109764.
[9] A.F. Hofmann, L.R. Hagey, Key discoveries in bile acid chemistry and biology and their clinical applications: History of the last eight decades, J. Lipid Res. 55 (8) (2014) 1553–1595, https://doi.org/10.1194/jlr.R049437.
[10] P. Terech, Y. Talmon, Aqueous suspensions of steroid nanotubules: Structural and rheological characterizations, Langmuir. 18 (19) (2002) 7240–7244, https://doi.org/10.1021/la025574r.
[11] J. Israelachvili, The science and applications of emulsions - an overview, Colloids Surfaces A Physicochem. Eng. Asp. 91 (1994) 1–8, https://doi.org/10.1016/0927-7757(94)02743-9.
[12] J. Israelachvili, Intermolecular and Surface Forces, Third Edition., Academic Press, Santa Barbara, 2011, 10.1016/C2009-0-21560-1.
[13] A. Jover, F. Fraga, F. Meijide, J. Vázquez Tato, J. Cautela, A. Del Giudice, M.C. di Gregorio, Revealing the complex self-assembly behaviour of sodium deoxycholate in aqueous solution, J. Colloid Interface Sci. 604 (2021) 415–428, https://doi.org/10.1016/j.jcis.2021.06.140.
[14] D.M. Blow, A. Rich, Studies on the Formation of Helical Deoxycholate Complexes, J. Am. Chem. Soc. 82 (1960) 3566–3571, https://doi.org/10.1021/ja01499a023.
[15] A. Jover, F. Meijide, E. Rodríguez Núñez, J. Vázquez Tato, Aggregation kinetics of sodium deoxycholate in aqueous solution, Langmuir. 14 (1998) 4359–4363, https://doi.org/10.1021/la9712754.
[16] A. Rich, D.M. Blow, Formation of a helical steroid complex, Nature. 182 (4633) (1958) 423–426, https://doi.org/10.1038/182423a0.
[17] H. Sobotka, N. Czeczowiczka, The gelation of bile salt solutions, J. Colloid Sci. 13 (2) (1958) 188–191, https://doi.org/10.1016/0095-8522(58)90024-2.
[18] A. Jover, F. Meijide, E. Rodríguez Núñez, J. Vázquez Tato, M. Mosquera, F. Rodríguez Prieto, Unusual pyrene excimer formation during sodium deoxycholate gelation, Langmuir. 12 (7) (1996) 1789–1793, https://doi.org/10.1021/la9506335.
[19] A. Jover, F. Meijide, E. Rodríguez Núñez, J. Vázquez Tato, Dynamic rheology of sodium deoxycholate gels, Langmuir. 18 (2002) 987–991, https://doi.org/10.1021/la011178h.
[20] P. Li, C. Malveau, X.X. Zhu, J.D. Wuest, Using Nuclear Magnetic Resonance Spectroscopy to Probe Hydrogels Formed by Sodium Deoxycholate, Langmuir. 38 (17) (2022) 5111–5118, https://doi.org/10.1021/acs.langmuir.1c0217510.1021/acs.langmuir.1c02175.s001.
[21] L. Ovesen, F. Bendtsen, U. Tage-Jensen, N.T. Pedersen, B.R. Gram, S.J. Rune, Intraluminal pH in the stomach, duodenum, and proximal jejunum in normal subjects and patients with exocrine pancreatic insufficiency, Gastroenterology. 90 (4) (1986) 958–962, https://doi.org/10.1016/0016-5085(86)90873-5.
[22] A.F. Hofmann, The continuing importance of bile acids in liver and intestinal disease, Arch. Intern. Med. 159 (1999) 2647–2658, https://doi.org/10.1001/archinte.159.22.2647.
[23] M.C. di Gregorio, J. Cautela, L. Galantini, Physiology and physical chemistry of bile acids, Int. J. Mol. Sci. 22 (2021) 1–23, https://doi.org/10.3390/ijms22041780.
[24] D. Fitzgerald, C. Du, S. Asaph, Technical Assessment of the Anton Paar DMA5000 density meter, United Kindom, 2000.
[25] A. Furtado, R. Pagel, F. Lorenz, I. Godinho, H. Wolf, Viscosity estimation of Newtonian liquids from data obtained by oscillation-type density meters 25 (2017) 321–328.
[26] A. Furtado, J. Gavina, A. Napoleão, J. Pereira, M.T. Cidade, J. Sousa, Density measurements of viscoelastic samples with oscillation-type density meters, J. Phys. Conf. Ser. 1379 (1) (2019) 012020, https://doi.org/10.1088/1742-6596/1379/1/012020.
[27] E.W. Lemmon, M.O. McLinden, D.G. Friend, Thermophysical properties of fluid systems., in: P.J. Linstrom, W.G. Mallard (Eds.), NIST Chem. WebBook, NIST Stand. Ref. Database Number 69, National Institute of Standards and Technology, Gaithersburg MD, 20899, USA, 1998. https://doi.org/10.18434/T4D303.
[28] A. Weissberger, J. Riddick, W. Bunger, T.K. Sakano, Techniques of chemistry. - 2: Organic solvents. Physical properties and methods of purification, 4.ed,., Wiley, New York, N.Y, 1986.
[29] A.R. Campanelli, S. Candeloro De Sanctis, E. Giglio, S. Petriconi, The structure of helices of rubidium deoxycholate–water (3/10), 3(Rb+.C24H39O4−).10H2O, Acta Crystallogr Sect. C Cryst. Struct. Commun. 40 (1984) 631–635, https://doi.org/10.1107/s010827018400514x.
[30] V.M. Coiro, E. Giglio, S. Morosetti, A. Palleschi, A monoclinic phase of the deoxycholic acid rubidium salt, Acta Crystallogr, Sect. B Struct. Crystallogr. Cryst. Chem. 36 (1980) 1478–1480, https://doi.org/10.1107/s0567740880006322.
[31] G.R. Pettit, J.C. Knight, D.L. Herald, R. Davenport, R.K. Pettit, B.E. Tucker, J.M. Schmidt, Isolation of labradorins 1 and 2 from Pseudomonas syringae pv. coronafaciens, J. Nat. Prod. 65 (12) (2002) 1793–1797, https://doi.org/10.1021/np020173x.
[32] K.R. Harris, M. Kanakubo, L.A. Woolf, Temperature and Pressure Dependence of the Viscosity of the Ionic Liquids 1-Methyl-3-octylimidazolium Hexafluorophosphate and 1-Methyl-3-octylimidazolium Tetrafluoroborate, J. Chem. & Eng. Data. 51 (3) (2006) 1161–1167, https://doi.org/10.1021/je060082s.
[33] K.R. Harris, L.A. Woolf, M. Kanakubo, Temperature and Pressure Dependence of the Viscosity of the Ionic Liquid 1-Butyl-3-methylimidazolium Hexafluorophosphate, J. Chem. & Eng. Data. 50 (5) (2005) 1777–1782, https://doi.org/10.1021/je050147b.
[34] S. Davidson, H. Joosten, H. Fitzgerald, Density measurement of viscous oils (using vibrating tube density meters), NPL Report ENG 39, United Kingdom, 2012.
[35] K. Fontell, Micellar behaviour in solutions of bile-acid salts 111. Viscosity und density measurements in the aqueous solutions, Kolloid-Z. u. Z. Polym. 246 (1) (1971) 614–625.
[36] R. Zana, Comments on the Paper "The Role of Hydrogen Bonding in the Formation of Bile Salt Micelles" by D. G. Oakenfull and L. R. Fisher, J. Phys. Chem. 82 (1978) 2240–2243.
[37] C. La Mesa, A. Khan, K. Fontell, B. Lindman, Phase diagrams and NMR studies of some ternary sodium deoxycholate-surfactant-water systems, J. Colloid Interface Sci. 103 (2) (1985) 373–391, https://doi.org/10.1016/0021-9797(85)90116-X.
[38] A. Maestre, P. Guardado, M.L. Moyá, Thermodynamic study of bile salts micellization, J. Chem. Eng. Data. 59 (2) (2014) 433–438, https://doi.org/10.1021/je400903n.
[39] P. Garidel, A. Hildebrand, R. Neubert, A. Blume, Thermodynamic characterization of bile salt aggregation as a function of temperature and ionic strength using isothermal titration calorimetry, Langmuir. 16 (12) (2000) 5267–5275, https://doi.org/10.1021/la9912390.
[40] A.A. D'Archivio, L. Galantini, E. Giglio, A. Jover, X-ray and quasi-elastic light-scattering studies of sodium deoxycholate, Langmuir. 14 (17) (1998) 4776–4781, https://doi.org/10.1021/la971312r.
[41] G. Conte, R. Di Blasi, E. Giglio, A. Parretta, N.V. Pavel, Nuclear magnetic resonance and X-ray studies on micellar aggregates of sodium deoxycholate, J. Phys. Chem. 88 (23) (1984) 5720–5724, https://doi.org/10.1021/j150667a052.
[42] A.R. Campanelli, D. Ferro, E. Giglio, P. Imperatori, V. Piacente, Thermal and X-ray study of sodium deoxycholate crystal and fibre, Thermochim. Acta. 67 (2-3) (1983) 223–232, https://doi.org/10.1016/0040-6031(83)80102-6.
[43] D.J. Cabral, J.A. Hamilton, D.M. Small, The ionization behavior of bile acids in different aqueous environments, J. Lipid Res. 27 (3) (1987) 334–343.
[44] P. Becher, Hydrophile-Lipophile Balance: History and Recent Developments, J. Dispers. Sci. Technol. 5 (1983) 81–96.
[45] Y. Moroi, M. Kitagawa, H. Itoh, Aqueous solubility and acidity constants of cholic, deoxycholic, chenodeoxycholic, and ursodeoxycholic acids, J. Lipid Res. 33 (1) (1992) 49–53.
[46] G. Deng, C. Tang, F. Li, H. Jiang, Y. Chen, Covalent cross-linked polymer gels with reversible sol-gel transition and self-healing properties, Macromolecules. 43 (3) (2010) 1191–1194, https://doi.org/10.1021/ma9022197.
[47] A. Jourdain, R. Asbai, O. Anaya, M.M. Chehimi, E. Drockenmuller, D. Montarnal, Rheological Properties of Covalent Adaptable Networks with 1,2,3-Triazolium Cross-Links: The Missing Link between Vitrimers and Dissociative Networks, Macromolecules. 53 (6) (2020) 1884–1900, https://doi.org/10.1021/acs.macromol.9b0220410.1021/acs.macromol.9b02204.s001.

[48] E.R. Morris, K. Nishinari, M. Rinaudo, Gelation of gellan - A review, Food Hydrocoll. 28 (2) (2012) 373–411, https://doi.org/10.1016/j.foodhyd.2012.01.004.
[49] H.P.S. Abdul Khalil, Y.Y. Tye, C.K. Saurabh, C.P. Leh, T.K. Lai, E.W.N. Chong, M.R. Nurul Fazita, J. Mohd Hafiidz, A. Banerjee, M.I. Syakir, Biodegradable polymer films from seaweed polysaccharides: A review on cellulose as a reinforcement material, Express Polym. Lett. 11 (4) (2017) 244–265, https://doi.org/10.3144/expresspolymlett.2017.26.
[50] P.R.A. Chivers, D.K. Smith, Shaping and structuring supramolecular gels, Nat. Rev. Mater. 4 (7) (2019) 463–478, https://doi.org/10.1038/s41578-019-0111-6.
[51] L.i. Zhang, X. Wang, T. Wang, M. Liu, Tuning soft nanostructures in self-assembled supramolecular gels: From morphology control to morphology-dependent functions, Small. 11 (9-10) (2015) 1025–1038, https://doi.org/10.1002/smll.201402075.
[52] D. Stauffer, A. Coniglio, M. Adam, Gelation and Critical Phenomena., in: Adv. Polym. Sci., Springer-Verlag, Berlin, 1982: pp. 103–158. https://doi.org/10.1007/3-540-11471-8_4.
[53] P.J. Flory, Molecular Size Distribution in Three Dimensional Polymers. I. Gelation, J. Am. Chem. Soc. 63 (1941) 3083–3090, https://doi.org/10.1021/JA01856A061.
[54] P.J. Flory, Molecular Size Distribution in Three Dimensional Polymers. II. Trifunctional Branching Units, J. Am. Chem. Soc. 63 (11) (1941) 3091–3096.
[55] P.J. Flory, Molecular size distribution in three dimensional polymers. III. Tetrafunctional branching units, J. Am. Chem. Soc. 63 (11) (1941) 3096–3100.
[56] W.H. Stockmayer, Theory of molecular size distribution and gel formation in branched-chain polymers, J. Chem. Phys. 11 (2) (1943) 45–55, https://doi.org/10.1063/1.1723803.
[57] T. Tanaka, Dynamics of critical concentration fluctuations in gels, Phys. Rev. A. 17 (2) (1978) 763–766, https://doi.org/10.1103/PhysRevA.17.763.
[58] T. Tanaka, Collapse of Gels and the Critical Endpoint, Phys. Rev. Lett. 40 (12) (1978) 820–823.
[59] M. Daoud, A. Coniglio, Singular behaviour of the free energy in the sol-gel transition, J. Phys. A. Math. Gen. 14 (8) (1981) L301–L306, https://doi.org/10.1088/0305-4470/14/8/008.
[60] A.N. Semenov, M. Rubinstein, Thermoreversible gelation in solutions of associative polymers. 1. Statics, Macromolecules. 31 (4) (1998) 1373–1385, https://doi.org/10.1021/ma970616h.
[61] T. Matsoukas, Statistical Thermodynamics of Irreversible Aggregation: The Sol-Gel Transition 8855(1–5) Sci. Rep. 5 (2015), https://doi.org/10.1038/srep088551.
[62] A. Coniglio, H.E. Stanley, W. Klein, Solvent effects on polymer gels: A statistical-mechanical model, Phys. Rev. B. 25 (11) (1982) 6805–6821, https://doi.org/10.1103/PhysRevB.25.6805.
[63] I. Erukhimovich, M.V. Thamm, A.V. Ermoshkin, Thermodynamic and Structural Characteristics of the Gel Phase (2001) 5653–5674.
[64] I. Erukhimovich, A.V. Ermoshkin, Phase diagrams classification of thermoreversibly associating systems with due regard for mesoscopic cyclization effects, J. Chem. Phys. 116 (2002) 368–383, https://doi.org/10.1063/1.1412866.
[65] F. Sciortino, E. Zaccarelli, Reversible gels of patchy particles, Curr. Opin. Solid State Mater. Sci. 15 (6) (2011) 246–253, https://doi.org/10.1016/j.cossms.2011.07.003.
[66] B. Wunderlich, Thermal analysis of polymeric materials, Springer, Berlin Heidelberg (2005), https://doi.org/10.1007/B137476.
[67] R.A. Gonçalves, Y.M. Lam, B. Lindman, Double-chain cationic surfactants: Swelling, structure, phase transitions and additive effects, Molecules. 26 (2021) 1–26, https://doi.org/10.3390/molecules26133946.
[68] R.A. Gonçalves, P. Naidjonoka, T. Nylander, M.G. Miguel, B. Lindman, Y.M. Lam, Facile control of surfactant lamellar phase transition and adsorption behavior, RSC Adv. 10 (31) (2020) 18025–18034.
[69] P.C. Schulz, DSC analysis of the state of water in surfactant-based microstructures, J. Therm. Anal. Calorim. 51 (1) (1998) 135–149, https://doi.org/10.1007/BF02719017.
[70] E.G. Merino, C. Rodrigues, M.T. Viciosa, C. Melo, J. Sotomayor, M. Dionísio, N.T. Correia, Phase transformations undergone by triton X-100 probed by differential scanning calorimetry and dielectric relaxation spectroscopy, J. Phys. Chem. B. 115 (43) (2011) 12336–12347, https://doi.org/10.1021/jp2028033.
[71] S. Kaneshina, M. Yamanaka, A differential scanning calorimetric study of the thermotropic phase behavior of surfactant assemblies in water, J. Colloid Interface Sci. 131 (2) (1989) 493–497, https://doi.org/10.1016/0021-9797(89)90191-4.
[72] M. Gubitosi, A. D'Annibale, K. Schillén, U. Olsson, N.V. Pavel, L. Galantini, On the stability of lithocholate derivative supramolecular tubules, RSC Adv. 7 (1) (2017) 512–517.
[73] M.C. di Gregorio, M. Gubitosi, L. Travaglini, N.V. Pavel, A. Jover, F. Meijide, J. Vázquez Tato, S. Sennato, K. Schillén, F. Tranchini, S. De Santis, G. Masci, L. Galantini, Supramolecular assembly of a thermoresponsive steroidal surfactant with an oppositely charged thermoresponsive block copolymer, Phys. Chem. Chem. Phys. 19 (2) (2017) 1504–1515.